

## Gd–Hydroxypyridinone (HOPO)-Based High-Relaxivity Magnetic Resonance Imaging (MRI) Contrast Agents

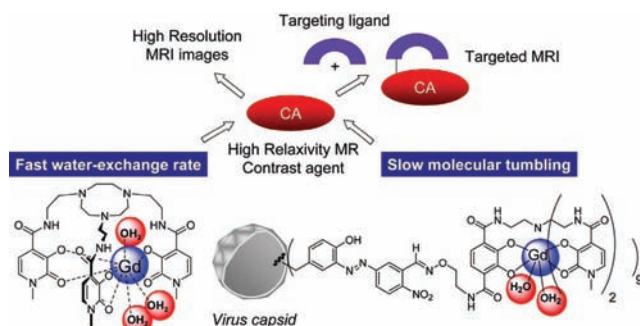
ANKONA DATTA AND KENNETH N. RAYMOND\*

Chemistry Department, University of California, Berkeley, California 94720

RECEIVED ON NOVEMBER 6, 2008

### CON SPECTUS

Magnetic resonance imaging (MRI) is a particularly effective tool in medicine because of its high depth penetration (from 1 mm to 1 m) and ability to resolve different soft tissues. The MRI signal is generated by the relaxation of *in vivo* water molecule protons. MRI images can be improved by administering paramagnetic agents, which increase the relaxation rates of nearby water protons, thereby enhancing the MRI signal. The lanthanide cation  $Gd^{3+}$  is generally used because of its favorable electronic properties; high toxicity, however, necessitates strongly coordinating ligands to keep  $Gd^{3+}$  completely bound while in the patient. In this Account, we give a coordination chemistry overview of contrast agents (CAs) based on Gd–hydroxypyridinone (HOPO), which show improved MRI contrast and high thermodynamic stabilities.



Tris-bidentate HOPO-based ligands developed in our laboratory were designed to complement the coordination preferences of  $Gd^{3+}$ , especially its oxophilicity. The HOPO ligands provide a hexadentate coordination environment for  $Gd^{3+}$ , in which all of the donor atoms are oxygen. Because  $Gd^{3+}$  favors eight or nine coordination, this design provides two to three open sites for inner-sphere water molecules. These water molecules rapidly exchange with bulk solution, hence affecting the relaxation rates of bulk water molecules. The parameters affecting the efficiency of these contrast agents have been tuned to improve contrast while still maintaining a high thermodynamic stability for  $Gd^{3+}$  binding. The Gd–HOPO-based contrast agents surpass current commercially available agents because of a higher number of inner-sphere water molecules, rapid exchange of inner-sphere water molecules via an associative mechanism, and a long electronic relaxation time. The contrast enhancement provided by these agents is at least twice that of commercial contrast agents, which are based on polyaminocarboxylate ligands.

Advances in MRI technology have made significant contributions to the improvement of clinical diagnostics by allowing visualization of underlying pathology. However, understanding the mechanism of a disease at the molecular level requires improved imaging sensitivity. The ultimate goal is to visually distinguish between different disease targets or markers, such as enzymes, hormones, proteins, or small molecules, at biologically relevant concentrations (from micro- to nanomolar). Although MRI techniques can provide images of the organs and tissues in which these biomarkers are regulated, the high sensitivity required to visualize the biological targets within the tissues is currently lacking; contrast enhancements of 50-fold beyond current agents are required to achieve this goal. According to the theory of paramagnetic relaxation, the contrast enhancement can be further improved by slowing the tumbling rate of the MRI agent. Theoretically, this enhancement would be greater for contrast agents with an optimal rate of water exchange. The Gd–HOPO-based contrast agents have optimal water-exchange rates, whereas the commercial agents have slower non-optimal water-exchange rates; thus, the Gd–HOPO agents are ideal for attachment to macromolecules, which will slow down the tumbling rate and increase contrast. This strategy has been recently tested with the Gd–HOPO agents via covalent attachment to virus capsids, affording contrast enhancements 10-fold beyond commercial agents.

## Introduction

Magnetic resonance imaging (MRI) is a frequently used diagnostic technique because it is non-invasive, able to differentiate between soft tissues, and has high lateral and depth resolutions.<sup>1–3</sup> The signal intensity in MRI depends upon the relaxation rates of water molecule protons. Differences in the environments of water molecules *in vivo* gives rise to the inherent contrast in MRI, however the contrast is sometimes not high enough to distinguish between normal and diseased tissues.<sup>4</sup> This inherent contrast can be improved by the administration of paramagnetic metal-ion-containing contrast agents, which affect the relaxation rates of nearby water molecules. Among the different paramagnetic metal ions ( $\text{Mn}^{2+}$ ,  $\text{Mn}^{3+}$ ,  $\text{Fe}^{3+}$ , and  $\text{Gd}^{3+}$ ) used in contrast agents,  $\text{Gd}^{3+}$  is most frequently used in commercial agents,<sup>5</sup> because of its seven unpaired electrons and long electronic relaxation time. Although  $\text{Gd}^{3+}$  provides excellent contrast, the high toxicity of the  $\text{Gd}^{3+}$  aqua ion necessitates the strong coordination of  $\text{Gd}^{3+}$  by organic chelators before *in vivo* use.<sup>6</sup> The contrast-enhancing capacity of  $\text{Gd}^{3+}$ -based contrast agents is directly proportional to the number of exchangeable water molecules in the inner coordination sphere of the  $\text{Gd}^{3+}$  ion. Unfortunately, the complexation of  $\text{Gd}^{3+}$  by organic chelators reduces the number of inner sphere water molecules and leads to low (millimolar) sensitivity. Hence, one of the major challenges in the field of Gd-based MRI contrast agents is to improve the contrast to obtain micro- to nanomolar sensitivities for molecular imaging while minimizing the toxic side effects of  $\text{Gd}^{3+}$ . Our work has focused on two aspects of this problem: (1) improving the stability of the Gd complexes to be used as contrast agents by developing ligands based on the coordination properties of  $\text{Gd}^{3+}$  and (2) maximizing contrast by tuning the parameters affecting signal intensity in MRI.

The measure of signal enhancement due to an MRI contrast agent is described by the term relaxivity, defined as the increase in the relaxation rate of water molecule protons per millimolar concentration of contrast agent applied. Gd-based contrast agents increase both the longitudinal ( $1/T_1$ ) and transverse ( $1/T_2$ ) relaxation rates of nearby water molecules. A greater increase is observed for the  $1/T_1$  relaxation rates in tissues; hence, Gd-based agents improve the contrast more in  $T_1$ -weighted images than in  $T_2$ -weighted images.<sup>5</sup> The relaxation of the inner-sphere water molecules through dipolar interactions contributes the most to the longitudinal relaxation rate increase for  $\text{Gd}^{3+}$ . According to the Solomon–Bloembergen–Morgan (SBM) equations, which model paramagnetic relaxivity, the dipolar contribution to the longitudinal relaxivity ( $r_{1p}$ )

can be maximized by increasing the number of inner-sphere water molecules ( $q$ ), optimizing the water-exchange rates ( $1/\tau_M$ , where  $\tau_M$  is the water residence lifetime) between the inner- and outer-sphere water molecules, and slowing the molecular tumbling rate ( $1/\tau_R$ , where  $\tau_R$  is the rotational correlation time) of the contrast agent (CA).<sup>7–10</sup> These equations also describe the field strength dependence of relaxivity.

Relaxivity values up to  $350 \text{ mM}^{-1} \text{ s}^{-1}$  are theoretically possible, at field strengths between 20–100 MHz, when  $q = 3$  and the electronic relaxation parameters are  $T_{1e} = 15 \text{ ns}$  and  $T_{2e} = 0.3 \text{ ns}$ . These high-relaxivity values will help achieve the sensitivity required for targeted imaging using MRI. Relaxivity values for current contrast agents are of the order of  $4\text{--}5 \text{ mM}^{-1} \text{ s}^{-1}$  (20 MHz),<sup>5</sup> which can be improved by tuning the parameters affecting relaxivity. Several attempts have been made at improving the commercial contrast agents, and these results are summarized in recent reviews.<sup>4,11–14</sup> Along with high-relaxivity values, targeted MRI also requires the design of “turn-on” or “responsive” sensors that can afford a signal intensity change upon an interaction with a biomarker of interest. Contrast agents that are responsive to pH, enzyme activity, and metal ions have been developed, and the reader is referred to several recent publications on these topics.<sup>15–19</sup>

Gd–hydroxypyridinone (HOPO)-based contrast agents have been developed using a rational design based on Gd coordination chemistry, and these compounds will be the focus of this Account. The mechanism of fast water exchange observed for these complexes will be reviewed, and its implications in obtaining high-relaxivity values will be discussed. Recently published work involving the attachment of these complexes to biomacromolecules to attain high-relaxivity values and insights obtained into the dependence of relaxivity upon molecular tumbling will also be reviewed. We will conclude with our perspective on strategies for attaining high sensitivity in MRI.

## Coordination Geometry Considerations in Designing Ligands for $\text{Gd}^{3+}$

**O versus N Donors.** Trivalent lanthanide ions, such as  $\text{Gd}^{3+}$ , usually exhibit variable coordination numbers of eight or nine.<sup>20</sup> Lanthanide ions earlier in the periodic table have ionic radii similar to  $\text{Ca}^{2+}$ , while the later lanthanides have ionic radii similar to  $\text{Mn}^{2+}$ . Because of this similarity, lanthanide ions can displace  $\text{Ca}^{2+}$  and  $\text{Mn}^{2+}$  from their binding sites in proteins and are used to elucidate the structures of proteins by X-ray crystallography and nuclear magnetic resonance (NMR) spectroscopy.<sup>21,22</sup> In a study by Pidcock and Moore, X-ray structures of  $\text{Ca}^{2+}$ - and lanthanide-ion-containing proteins and

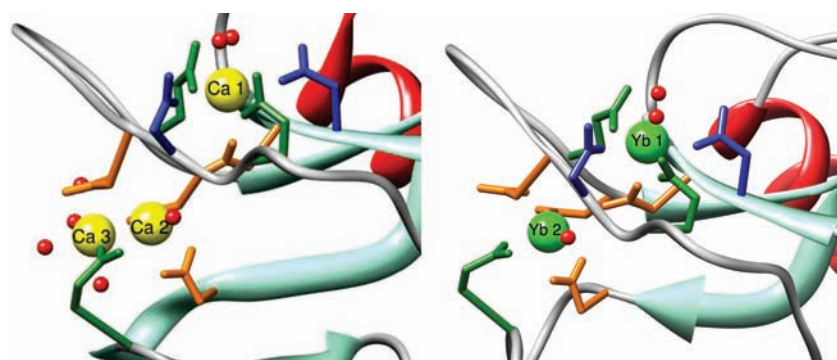


**FIGURE 1.** Learning from nature: comparison of active sites in a mannose-binding protein that recognizes high mannose concentrations on pathogenic cell surfaces. (Left) Native rat mannose-binding protein A (resolution of 1.95 Å)<sup>24</sup> showing a close-up view of the Ca<sup>2+</sup>-binding sites. The color coding is green for Glu, orange for Asp, and blue for Asn. (Right) Yb<sup>3+</sup>-substituted subtilisin fragment of the same protein (resolution of 1.80 Å)<sup>23</sup> showing a close-up view of the metal-binding site. The same ligands binding the Ca<sup>2+</sup> ions also bind the Yb<sup>3+</sup> ions (Yb1 is in the Ca1 site, and Yb2 is in the site for Ca2/3).

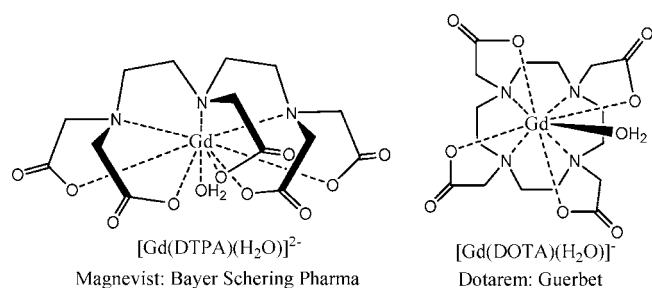


**FIGURE 2.** Two representative Gd<sup>3+</sup> polyaminocarboxylate-based commercial contrast agents with one inner-sphere water molecule in each.

coordination complexes were compared to find the similarities between the structural features of the metal-binding sites.<sup>21</sup> The average coordination number for Ca<sup>2+</sup> in a protein is 6.0 (remaining ligands could be water molecules), while the average coordination number of a Ln<sup>3+</sup> ion in an intrinsic protein Ca<sup>2+</sup> site was found to be ca. 7.2. Oxygen atoms bind more strongly than nitrogen atoms in the coordination sites, with carboxylates (aspartates and glutamates) being the most common. A comparison of two crystal structures of a mannose-binding protein is shown in Figure 1, depicting the Ca<sup>2+</sup> sites in the native protein. Yb<sup>3+</sup> binds to the oxygen-donor-rich intrinsic Ca<sup>2+</sup>-binding sites.<sup>23,24</sup> This similarity in the binding environments between Ca<sup>2+</sup> and lanthanides was also used in a recent study, in which the Ca<sup>2+</sup>-binding sites in a CCMV virus were filled with Gd<sup>3+</sup> to create macromolecular MRI contrast agents.<sup>25</sup> Thus, in designing ligands for Gd<sup>3+</sup>, the structural features of natural Ca<sup>2+</sup>-binding sites can be incorporated and should lead to higher stabilities.

The current commercially available contrast agents are based on polyaminocarboxylate ligands (Figure 2), which incorporate both nitrogen and oxygen donors.<sup>12,26</sup> These ligands are octadentate and leave one coordination site open for binding water molecules. The high ligand denticity is

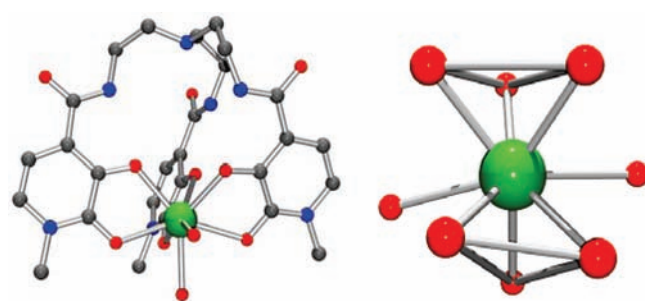


**FIGURE 3.** (Left) X-ray crystal structure of Gd-TREN-1-Me-3,2-HOPO (**1**) and (Right) the coordination polyhedron. The polyhedron is close to a tricapped trigonal prism, with the missing ligand position pointing directly toward the reader.<sup>27</sup>

needed to maintain complex stability, but the low number of inner-sphere water molecules compromises relaxivity. On the basis of the known oxophilicity of Gd<sup>3+</sup>, ligands containing only oxygen donors with lower denticity should offer high stability with low coordination numbers. This coordination preference of Gd<sup>3+</sup> was our guiding principle in designing the tris-bidentate HOPO-based complexes. These complexes incorporate six oxygen donors for Gd<sup>3+</sup> binding, leaving two to three coordination sites open for binding inner-sphere water molecules. The first HOPO-based ligand synthesized comprised of three bidentate HOPO moieties attached via a tris (2-aminoethyl) amine (TREN) cap. The Gd-TREN-1-Me-3,2-HOPO (**1**) complex has a relaxivity value of 10.5 mM<sup>-1</sup> s<sup>-1</sup> (at 20 MHz), almost twice that of commercial contrast agents. This is most likely a result of the higher number of inner-sphere water molecules.<sup>27</sup> The X-ray structure of this complex confirms that the hexadentate ligand binds gadolinium through the HOPO oxygen atoms, with two water molecules completing the coordination sphere (left panel of Figure 3).

The stability of a Gd complex is directly related to the concentration of free Gd<sup>3+</sup> *in vivo*, and different Gd complexes can be compared in terms of their pM values.<sup>28</sup> The Gd-TREN-

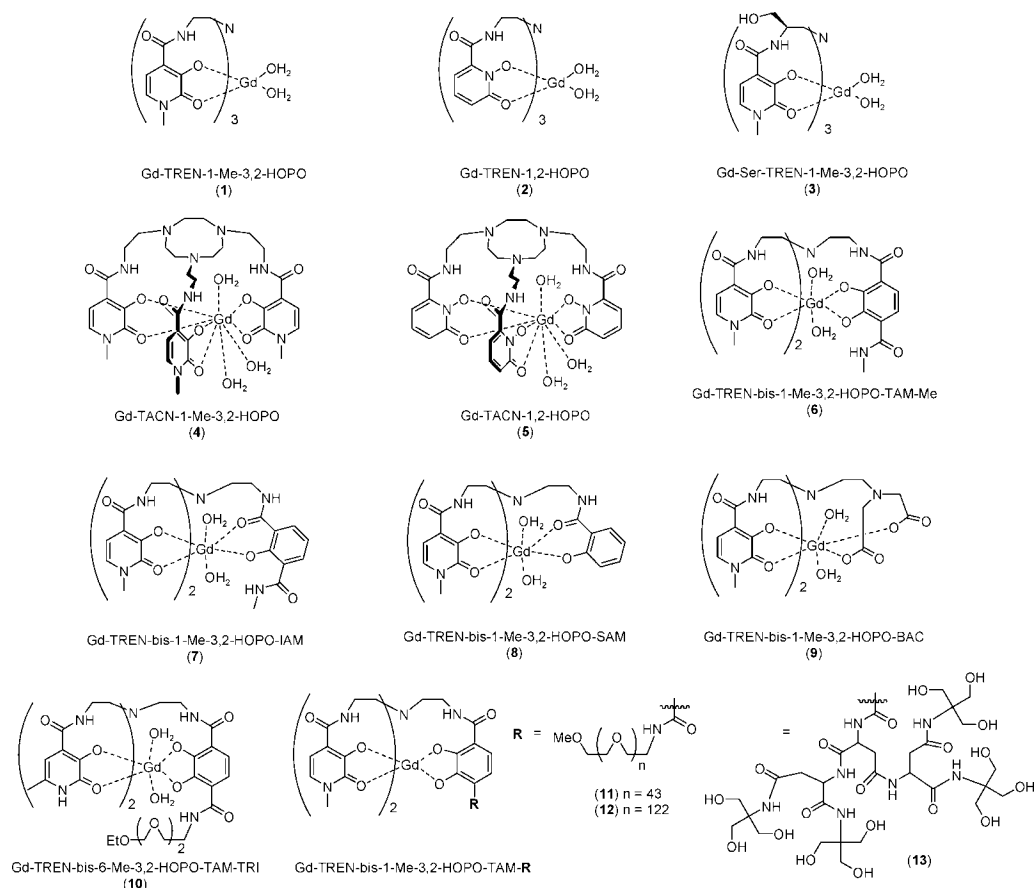


**FIGURE 4.** Chemical representations of the  $\text{Gd}^{3+}$  hydroxypyridinone complexes discussed in this paper.

1-Me-3,2-HOPO (**1**) complex exhibits a pM value of 20.3 at pH 7.4 [commercial agent Gd(DTPA) (Figure 2) has a pM value of 19.09]. For a detailed comparison of stability constants of Gd–HOPO-based complexes with current commercial contrast agents, the reader is referred to a recent review by our group.<sup>29</sup> The low solubility ( $\sim 1$  mM) of the Gd-TREN-1-Me-3,2-HOPO complex prompted the synthesis of a series of heteropodal ligands. Ligand cap variation was also explored. The most recent variation was replacing the TREN cap with a triazacyclononane (TACN)-based cap.<sup>30</sup> The HOPO complexes relevant to this Account are listed in Figure 4. The Gd-TACN-1-Me-3,2-HOPO complex (**4**) has solubility as high as 100 mM, maintains a reasonably high pM value of 18.7, and has a high-relaxivity value of  $13.1 \text{ mM}^{-1} \text{ s}^{-1}$  (20 MHz, 298 K).<sup>30</sup>

**Effect of Geometry and Coordination Number on the Mechanism of Water Exchange.** The early lanthanide aqua complexes ( $\text{La}^{3+}$ – $\text{Nd}^{3+}$ ) are nine-coordinate, while the smaller mid to late lanthanides ( $\text{Gd}^{3+}$ – $\text{Lu}^{3+}$ ) are eight-coordinate;  $\text{Sm}^{3+}$  and  $\text{Eu}^{3+}$  aqua ions exist in equilibria between eight- and nine-coordinate species.<sup>20</sup> The water-exchange process proceeds through either an associative mechanism, a dissociative mechanism, or an interchange mechanism between

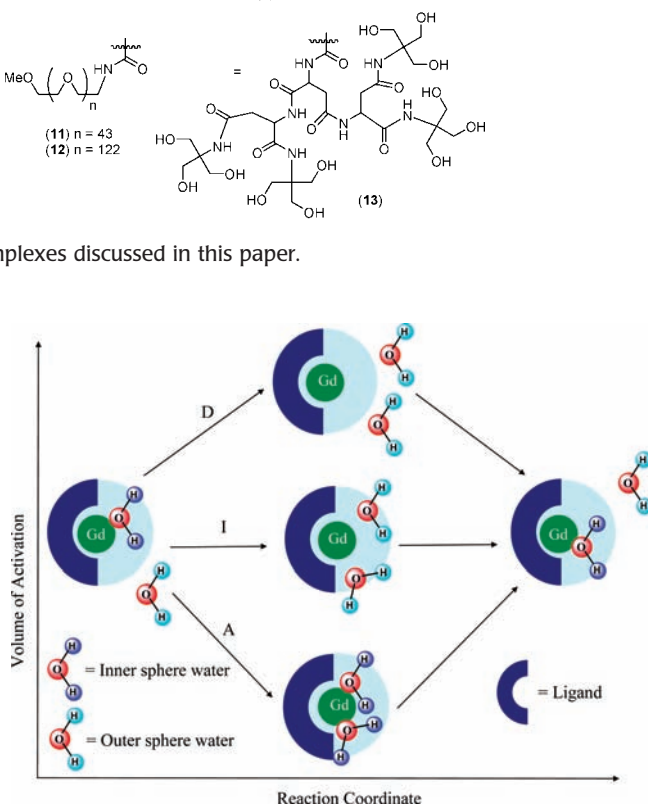


**FIGURE 5.** Representation of the transition states for the water-exchange processes possible for  $\text{Gd}^{3+}$  on the reaction coordinate.<sup>20</sup> Associative, interchange, and dissociative mechanisms are depicted in order of increasing volumes of activation.

associative and dissociative (Figure 5). Variable pressure  $^{17}\text{O}$  NMR measurements can be used to measure the volume of activation ( $\Delta V^\ddagger$  in the equation  $[\delta \ln(k_{\text{ex}})/\delta P]_{\text{T}} = -\Delta V^\ddagger/RT$ , where  $k_{\text{ex}}$  is the water-exchange rate) for the exchange process. A large negative  $\Delta V^\ddagger$  value indicates an associative

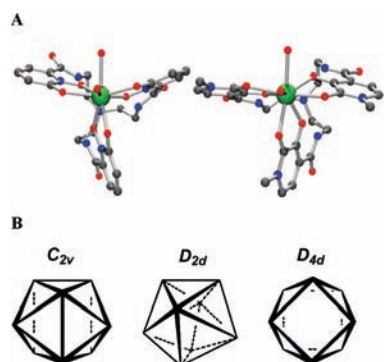


**FIGURE 6.** (A) Crystal structures for Gd-TREN-1,2-HOPO (**2**) (left) and Gd-TREN-1-Me-3,2-HOPO (**1**) (right), showing the subtle differences in the coordination polyhedron. (B) Ideal polyhedron to which the crystal structures can be compared to by using shape analysis. The  $S$  value is the lowest for comparison to  $C_{2v}$  for Gd-TREN-1,2-HOPO and for comparison to  $D_{2d}$  for Gd-TREN-1-Me-3,2-HOPO.<sup>33</sup>

mechanism; a large positive  $\Delta V^\ddagger$  value indicates a dissociative mechanism.<sup>20</sup> The  $Gd^{3+}$  aqua ion has a small negative volume of activation, indicating an associative interchange water-exchange mechanism through a nine-coordinate transition state.<sup>31</sup> The commercial polyaminocarboxylate-based ligands have nine-coordinate geometries for all lanthanides,<sup>35</sup> and these complexes exchange water through a dissociative process.<sup>31</sup>

The X-ray structure of Gd-TREN-1-Me-3,2-HOPO (**1**) shows an eight-coordinate complex, which indicates the possibility of an associative water-exchange mechanism.<sup>27</sup> The energy difference between the different coordination geometries is very small for lanthanides, and shape measure,  $S$ , is used to determine which ideal geometry the complex resembles.<sup>32</sup> The shape measure is defined as  $S = \min[\{(1/m)\sum_{i=1}^m(\delta_i - \theta_i)^2\}^{1/2}]$ , where  $m$  is the number of edges,  $\delta_i$  is the dihedral angle along the  $i^{\text{th}}$  edge of the experimental structure (the angle between normals of adjacent faces), and  $\theta_i$  is the dihedral angle along the  $i^{\text{th}}$  edge of the ideal comparison polyhedron. The structure of an eight-coordinate lanthanide complex can resemble one of the following high-symmetry polyhedra: the bicapped trigonal prism ( $C_{2v}$ ), trigonal dodecahedron ( $D_{2d}$ ), or square antiprism ( $D_{4d}$ ) (Figure 6). Because  $S$  is a true metric, the lowest value of  $S$  for the three pairs represents the best fit to the nearest idealized geometry. The crystal structure of Gd-TREN-1-Me-3,2-HOPO (**1**) is best described as a trigonal dodecahedron. There is an obvious hole in the coordination sphere of the structure, suggesting an open site for binding an additional water molecule (right panel of Figure 3). The crystal structure of Gd-TREN-1,2-HOPO (**2**) also conforms to an eight-coordinate gadolinium, with the shape measure suggesting a trigonal bicapped prism ( $C_{2v}$ ) (Figure 6).<sup>33</sup> Because there

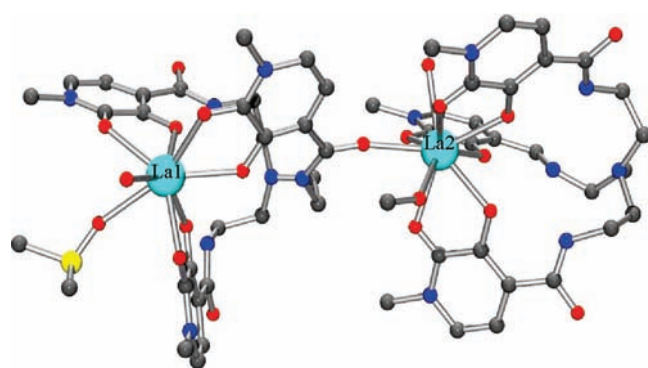


**FIGURE 7.** X-ray crystal structure of La-TREN-1-Me-3,2-HOPO, depicting the eight- and nine-coordinate  $La^{3+}$ -binding sites.<sup>34</sup>

is a small energy difference between the eight- and nine-coordinate geometries for lanthanides, these crystal structures suggest an associative mechanism for water exchange. Additionally, the crystal structure of TREN-1-Me-3,2-HOPO with  $La^{3+}$  has both an eight-coordinate (square antiprismatic) and a nine-coordinate (monocapped square antiprismatic) lanthanide metal center in the unit cell (Figure 7).<sup>34</sup> The presence of both eight- and nine-coordinate lanthanum TREN-1-Me-3,2-HOPO validates that the eight- and nine-coordinate geometries are indeed very close in energy, which should allow facile interconversion between the two coordination states. Finally, the small negative volume of activation ( $\Delta V^\ddagger = -5 \pm 1 \text{ cm}^3 \text{ mol}^{-1}$ ) for Gd-TREN-bis(6-Me-HOPO)-(TAM-TRI) (**10**) confirms an associative interchange mechanism similar to the gadolinium aqua ion ( $k_{\text{ex}} = 10.6 \times 10^8 \text{ s}^{-1}$ ).<sup>35</sup>

Analysis of the SBM equations shows that water-exchange rates of the order of  $10^8 \text{ s}^{-1}$  are near optimal for attaining high-relaxivity values (for field strengths between 20 and 100 MHz) upon slowing the tumbling motion.<sup>5</sup> Also, the small energy gap between the eight- and nine-coordinate species for the Gd–HOPO complexes, implied by the structures, means that tuning the ligand structure to stabilize the nine-coordinate species ( $q = 3$ ) is possible. Because  $q$  is directly proportional to relaxivity, this should increase relaxivity while maintaining stability. This gives the Gd–HOPO-based complexes an advantage over the commercial polyaminocarboxylate-based complexes, which can only equilibrate between  $q = 1$  (nine-coordinate) and  $q = 0$  (eight-coordinate) states.<sup>4</sup>

## Measurement of Water-Exchange Rates and Implications for Development of High-Relaxivity CA

The water-exchange rates for the Gd–HOPO complexes can be determined by variable-temperature proton-decoupled  $^{17}\text{O}$  NMR measurement of the water nuclear transverse relaxation

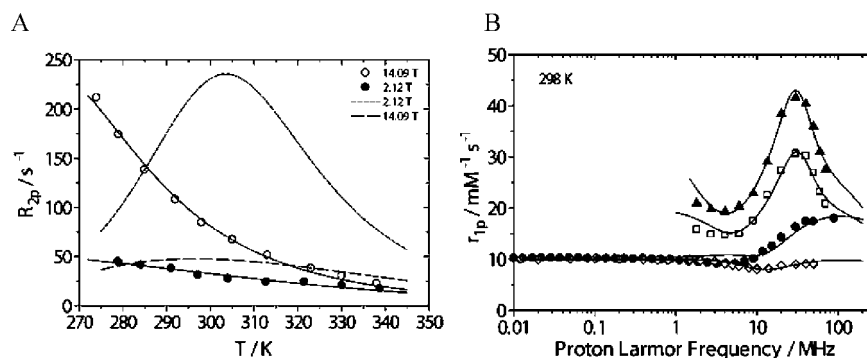


**FIGURE 8.** Representative plots of the typical relaxometric measurements performed for the Gd–HOPO complexes. (A)  $^{17}\text{O}$  NMR data for Gd-TREN-bis(6-Me-HOPO)-(TAM-TRI) (**10**) ( $\circ$  and  $\bullet$ ) and simulated curves for GdDO3A (Prohance), a commercial contrast agent (---).<sup>35,50</sup> (B) NMRD profiles and fits for Gd–HOPO-based macromolecular CAs obtained by conjugation of Gd-bis-HOPO-TAM to the interior of a virus capsid (**16**) ( $\blacktriangle$ ), exterior of a virus capsid (**15**) ( $\square$ ), and an aspartate-based dendrimer (**13**) ( $\bullet$ ). NMRD for the small-molecule CA Gd-TREN-bis(1-Me-3,2-HOPO)-TAM (**6**) is shown for comparison ( $\diamond$ ).<sup>38,39</sup>

rates (Figure 8A).<sup>34,35</sup> The more soluble heteropodal complexes (**6–10**) were used because high concentrations are required for these measurements. The data indicate fast water-exchange rates on the order of  $10^8 \text{ s}^{-1}$  (water residence lifetimes  $\tau_M = 10\text{--}15 \text{ ns}$ ), 1 order of magnitude slower than the  $\text{Gd}^{3+}$  aqua ion but 1–2 orders of magnitude faster than the polyaminocarboxylate-based complexes.

An estimate of the water-exchange rate can also be obtained by analyzing the temperature dependence of the longitudinal relaxivity.<sup>36</sup> Three different exchange regimes are possible: rapid water-exchange indicated by a relaxivity value increase with decreasing temperature (water-exchange rate is not the limiting factor determining relaxivity), slow exchange indicated by a relaxivity value decrease with decreasing temperature (water-exchange rate is limiting), and intermediate exchange indicated by little or no dependence of relaxivity upon temperature. The Gd–HOPO complexes (**6–8** and **10**) studied showed an exponential increase in relaxivity with decreasing temperature, indicating fast water exchange, with lifetimes ( $\tau_M$ ) well below 100 ns.<sup>34,35</sup>

Several modifications were made to HOPO-based complexes to increase their water solubility. Two major routes were synthesis of heteropodal terephthalamide (TAM) containing ligands bearing water-soluble substituents, for example, polyethyleneglycol (PEG) chains, and replacing the TREN backbone with more soluble caps.  $^{17}\text{O}$  NMR measurements on these more soluble systems gave a range for water residence lifetimes between 2 and 50 ns. The Gd-TREN-bis-HOPO-TAM complexes with PEG substituents (**11** and **12**) showed decreasing water-exchange rates with increasing PEG chain length ( $\tau_M = 19 \text{ ns}$  for **11** and  $31 \text{ ns}$  for **12**).<sup>37</sup> The field dependence of relaxivity, also known as the nuclear magnetic resonance dispersion (NMRD) profile, allows estimation of  $\tau_M$ ,  $q$ , and  $\tau_R$  when fitted to a model describing the magnetic coupling of

the solvent with the paramagnetic agent. Representative NMRD profiles for Gd–HOPO complexes are shown in Figure 8B.<sup>38,39</sup>  $q$  values of 1 were determined by  $^{17}\text{O}$  NMR and NMRD profiles for the PEG-substituted Gd-TREN-bis-HOPO-TAM complexes (**11** and **12**). The low  $q$  values are indicative of partial displacement of the inner-sphere water molecules by the PEG oxygen atoms. Because the water-exchange rate of associatively exchanging complexes depends upon the water concentration, lowering of the local water concentration caused by the PEG chain leads to a decrease in the water-exchange rate.

Replacement of the TREN backbone with a 2-hydroxyethyl-TREN cap (compound **3** in Figure 4) improves the water solubility and keeps the relaxivity similar to that of the original Gd-TREN-1-Me-3,2-HOPO complex.<sup>40,41</sup> Water exchange remains fast, and the water residence lifetime is 14 ns. Recently, the TREN cap was replaced with a TACN cap, which significantly improves the water solubility and gives a faster water-exchange rate ( $\tau_M = 2 \text{ ns}$ ).<sup>30</sup> Molecular mechanics models developed to calculate  $q$  from the exposed metal surface area and the strain energy of adding additional inner-sphere water molecules predict a  $q$  of 3 for the Gd-TACN-1-Me-3,2-HOPO complex (**4**).<sup>30,42</sup> The NMRD profiles of the Gd-complexes (**4** and **5**) and luminescence lifetime measurements on the  $\text{Eu}^{3+}$  version of TACN-1,2-HOPO confirm the predictions made by the modeling studies. These results indicate that the TACN-HOPO-based ligands stabilize nine-coordinate gadolinium ions and exchange the inner-sphere water molecules by a fast dissociative exchange mechanism. The fast water-exchange rate and the dissociative mechanism of exchange make the TACN-based complexes ideal for attachment to macromolecules to attain high-relaxivity values by slowing tumbling rates. A dissociative water-exchange mechanism should not depend upon the local water concentration, and hence, attachment to macromolecules should not decrease the water-

exchange rates, as in the case of the PEG-substituted TREN complexes (**11**, **12**).

## MR Contrast Enhancement upon Slowing Tumbling Rates

The optimum water-exchange rate for high relaxivity is field-strength-dependent. At the current clinically relevant MRI field strength (60 MHz), the optimum value for the water-residence lifetime is 10–30 ns (water-exchange rate around  $10^8 \text{ s}^{-1}$ ). With the advent of new high-field (100 MHz and greater) clinical scanners, the optimal water residence time would be around 1 ns (water-exchange rate close to that of the  $\text{Gd}^{3+}$  aqua ion,  $10^9 \text{ s}^{-1}$ ).<sup>29</sup>

Commercial  $\text{Gd}^{3+}$  polyaminocarboxylate-based complexes have water-exchange rates on the order of  $10^6 \text{ s}^{-1}$ , 2 orders of magnitude slower than the optimum water-exchange rate.<sup>31</sup> The contrast enhancement that can be obtained upon slowing the motion of these contrast agents is limited. Numerous studies have reported the attachment of the polyaminocarboxylate-based ligands to macromolecules, such as PEG chains, polymers, dendrimers, and nanoparticles, to slow the tumbling rate of the CA. Moderate enhancements in relaxivities have been observed for these systems, and the interested reader is referred to current reviews.<sup>4,11,43</sup> A notable result of these studies is that the water-exchange rate usually changes after attachment to the macromolecule. The factors responsible for this are the effect of the macromolecule on the local water concentration near the Gd center and the structural modifications on the ligand required to create the attachment point for the macromolecule. For example, the water residence lifetime of Gd–DTPA (Figure 2) is 300 ns. Upon attachment to polymers to form alkyl-DTPA-bisamide copolymers of the formula  $[\text{Gd}(\text{DTPA-BA})-(\text{CH}_2)_n]_x$ , the water residence times become longer ( $\tau_M = 2300$ , 1500, and 2000 ns for  $n = 6$ , 10, and 12, respectively).<sup>44</sup> For this set of polymers, the proton relaxivities were limited by the slow rates of water exchange. Similarly for Gd–DOTA (Figure 2) ( $\tau_M = 244$  ns), attached to a lysine-based dendrimer (Gadomer 17), the water residence time increased to 1000 ns, limiting the relaxivity to  $16.5 \text{ mM}^{-1} \text{ s}^{-1}$  (20 MHz).<sup>3</sup>

The Gd–HOPO-based contrast agents have water-residence times ( $\tau_M = 2\text{--}30$  ns) ideal for current and future high-field instruments. Additionally, the water exchange is not significantly slowed by conjugation to macromolecules. In the case of Gd–TREN-bis-1-Me-3,2-HOPO-TAM-based contrast agents with attached PEG chains (compounds **11** and **12**), the water residence times increased to 30 ns from 10 ns in the small-molecule contrast agent.<sup>37,45</sup> The water-exchange rate was still rapid enough that the relaxivity enhancements obtained

from these complexes were not limited by the water-exchange rate. This was also demonstrated by the temperature dependence of relaxivity, which decreased with increasing temperature. Attachment of Gd–TREN-bis-1-Me-3,2-HOPO-TAM to a small aspartate-based dendrimer (compound **13**) (molecular weight of 1576 g/mol) gave a relaxivity value of  $14.3 \text{ mM}^{-1} \text{ s}^{-1}$  (20 MHz), with  $^{17}\text{O}$  NMR studies indicating optimum water residence time ( $\sim 10$  ns).<sup>38</sup> Studies comparing Gd–HOPO complexes to commercial agents, performed by attaching multiple Gd–HOPO-based agents to dendrimers and other macromolecules, have been limited because of the low water solubility of the TREN-based contrast agents. One way to address this solubility issue is to attach the contrast agents to the interior of a soluble macromolecule with pores for water access. If the macromolecule has modifiable interior and exterior surfaces, then the exterior surface can be modified with targeting ligands and the interior surface can contain the Gd–HOPO-based agents.

Virus capsids have been recently explored as macromolecular scaffolds for attachment of MRI contrast agents.<sup>25,46,47</sup> We chose MS2 virus capsids as the soluble protein-based macromolecules to attach our Gd–HOPO-based contrast agents.<sup>39,48</sup> The MS2 capsid shell consists of 180 copies of a coat protein (molecular weight of 13.7 kDa) assembled in an icosahedral arrangement.<sup>49</sup> The RNA can be removed by treating the capsids with base to yield 27 nm diameter protein shells.<sup>48</sup> These capsid shells have 1.8 nm pores, through which small molecules and water can access the interior. The size of the capsids is ideal for imaging non-nervous system tissue, such as lesions in blood vessels and tumor tissues.<sup>39</sup> A total of 90 of the modified ligands **14** were attached to the externally modified capsids (Figure 9).<sup>48</sup> Attachment of more ligands caused the capsids to precipitate. The same number of ligands were attached to the internally modified capsids for comparison, and both the internal and external conjugates were complexed with  $\text{Gd}^{3+}$ . Relaxivity measurements for the capsid conjugates gave relaxivity values as high as  $41.6 \text{ mM}^{-1} \text{ s}^{-1}$  (per gadolinium;  $3952 \text{ mM}^{-1} \text{ s}^{-1}$  per particle, 30 MHz, 298 K) for the internal conjugates and  $30.7 \text{ mM}^{-1} \text{ s}^{-1}$  (per gadolinium;  $2548 \text{ mM}^{-1} \text{ s}^{-1}$  per particle, 30 MHz, 298 K) for the external conjugates. These high-relaxivity values indicate facile water diffusion into the interior of the capsids. The temperature dependence of relaxivity (increase in relaxivity with a decreasing temperature) indicates fast water exchange.

The NMRD profiles for these conjugates were fitted using the Lipari–Szabo model describing the rotational dynamics.<sup>39</sup> This model distinguishes between the two types of motions that influence proton relaxation: the local motion of

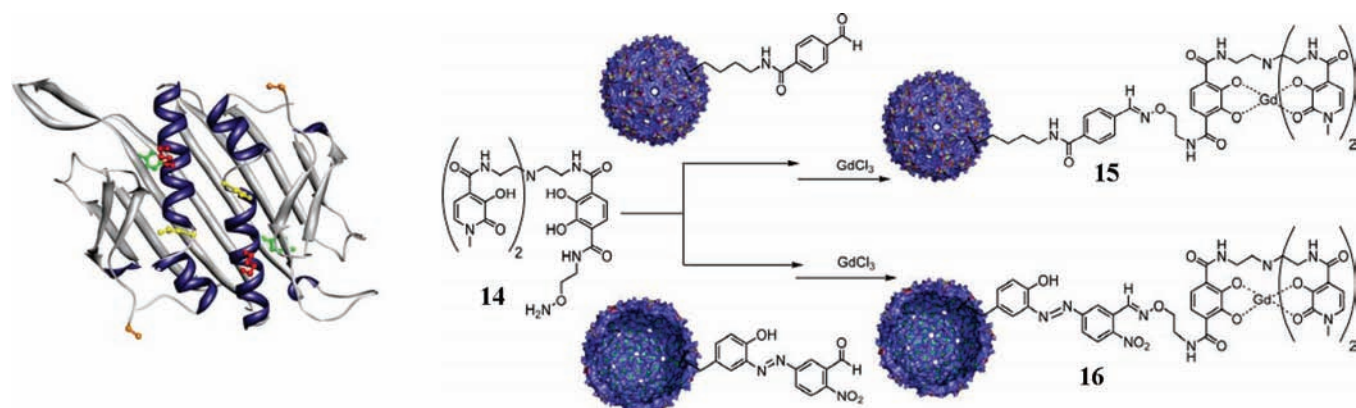


**FIGURE 9.** Attachment of Gd-TREN-bis(1-Me-3,2-HOPO)-TAM to bacteriophage MS2 capsids. The crystal structure of the coat protein dimer<sup>49</sup> (left) is shown with the modified residues highlighted. Tyr85 (green) in the interior, Lys106 (red) and Lys113 (yellow) on the exterior, and the N terminus (orange) are shown. The reaction of the ligands with the capsids to attach Gd complexes to the internally and externally modified capsids is shown in the scheme on the right.<sup>39,48</sup>

the contrast agent with a local correlation time  $\tau_{\text{RI}}$  and the global motion of the macromolecule with a global correlation time  $\tau_{\text{RG}}$ . Additionally, there is a parameter ( $S^2$ ) describing the efficiency of the coupling of the local and global motions ( $S^2 = 1$  when the CA rotates with the macromolecule, and  $S^2 = 0$  when the local motion of the CA is totally independent of the motion of the macromolecule). The best fits for the NMRD profiles were obtained with a  $\tau_{\text{M}}$  value of 10 ns (values between 2 and 20 ns were used for fitting the data), which is optimal for attaining high relaxivities. Although relaxivity values as high as  $40 \text{ mM}^{-1} \text{ s}^{-1}$  were obtained, these values were still lower than the theoretically predicted maximum relaxivity values. These results can be explained if we examine the parameters describing the motion of the system. For both the internal and external conjugates, the  $S^2$  values were low ( $S^2 = 0.08$  for external conjugates, and  $S^2 = 0.13$  for the internal conjugates at 298 K), with a slightly higher value for the internal conjugates. The  $\tau_{\text{RI}}$  value was also higher for the internal conjugates ( $\tau_{\text{RI}} = 0.44$  ns) than for the external conjugates ( $\tau_{\text{RI}} = 0.31$  ns). These results indicate that the rotation of the internally attached contrast agents is more closely linked to the capsid rotation than externally attached agents. This difference seems to translate into higher relaxivity for the internal conjugates. The internal conjugates were obtained by tyrosine modification (Y85 is located on a  $\beta$  sheet), while the external conjugates were obtained by lysine modifications (K106 and K113 are located on  $\alpha$  helices), and hence, internal conjugate flexibility is less than the external conjugate. Theoretical calculations on these systems indicate that higher  $\tau_{\text{RI}}$  values (3–15 ns), with optimum water-exchange rates, can give relaxivity values as high as  $140 \text{ mM}^{-1} \text{ s}^{-1}$  at 30 MHz.<sup>39</sup> At higher field strengths,  $\text{Gd}^{3+}$  complexes with faster water-exchange rates will be necessary to attain similar relaxivity

values.<sup>29</sup> TACN-based complexes are well-suited for this purpose. One of the current goals of the group is to attach the more soluble TACN-based ligands to macromolecules.

## Summary and Outlook

Hydroxypyridonate-based CAs designed to take advantage of the coordination preferences of  $\text{Gd}^{3+}$  have a large number of inner-sphere water molecules and fast water-exchange rates, requisite characteristics for high relaxivity. These ligands have only oxygen donor atoms, resulting in high thermodynamic stability for gadolinium binding. Slowing the tumbling rates of these CAs by attaching them to macromolecules has resulted in high-relaxivity complexes. In moving toward the next generation of high-relaxivity contrast agents for molecular imaging, these CAs could play an important role provided that water-solubility issues are resolved and high kinetic stability for gadolinium binding is also achieved. The ability to attach these contrast agents to the interior of virus capsid shells and the resultant high-relaxivity values have opened an avenue for targeted imaging via the attachment of ligands and receptors to the exterior of the capsids. These developments in MRI CAs in conjunction with improved imaging instruments should help bring targeted imaging closer to the clinic.

*We thank all of our co-workers and collaborators for their contributions to this project. We thank Prof. Mauro Botta for providing figures of NMRD profiles for this paper. This work was supported by National Institutes of Health (NIH) Grant HL69832, the Director, Office of Science, Office of Basic Energy Sciences, and the Division of Chemical Sciences, Geosciences, and Biosciences of the U.S. Department of Energy at Lawrence Berkeley National Laboratory (LBNL) under Contract DE-AC02-05CH11231.*



## BIOGRAPHICAL INFORMATION

**Ankona Datta** received her B.Sc. and M.Sc. degrees in chemistry from the Indian Institute of Technology, Kharagpur, in 2000, and her Ph.D. degree under Prof. John T. Groves from Princeton University in 2006. She is currently a postdoctoral scholar with Prof. Kenneth Raymond at University of California, Berkeley, developing macromolecular MRI contrast agents.

**Kenneth N. Raymond** is Chancellor's Professor at the University of California, Berkeley. He received his B.A. degree from Reed College in 1964 and his Ph.D. degree from Northwestern University in 1967, after which he began his faculty appointment at University of California, Berkeley. His research interests encompass microbial iron transport, the development of actinide sequestration agents, lanthanide-based luminescent and MRI agents, and supramolecular metal complex clusters for host–guest chemistry and catalysis.

## FOOTNOTES

\* To whom correspondence should be addressed. E-mail: raymond@socrates.berkeley.edu.

## REFERENCES

- Lauffer, R. B. Paramagnetic metal complexes as water proton relaxation agents for NMR imaging—Theory and design. *Chem. Rev.* **1987**, *87* (5), 901–927.
- The Chemistry of Contrast Agents in Medical Magnetic Resonance Imaging*; Merbach, A. E., Tóth, E., Eds.; Wiley: Chichester, U.K., 2001.
- Toth, E.; Helm, L.; Merbach, A. E. Relaxivity of MRI contrast agents. *Top. Curr. Chem.* **2002**, *221*, 61–101.
- Caravan, P. Strategies for increasing the sensitivity of gadolinium based MRI contrast agents. *Chem. Soc. Rev.* **2006**, *35* (6), 512–523.
- Caravan, P.; Ellison, J.; McMurry, T.; Lauffer, R. Gadolinium(III) chelates as MRI contrast agents: Structure, dynamics, and applications. *Chem. Rev.* **1999**, *99* (9), 2293–2352.
- Kumar, K.; Tweedle, M. F. Macrocyclic polyaminocarboxylate complexes of lanthanides as magnetic resonance imaging contrast agents. *Pure Appl. Chem.* **1993**, *65* (3), 515–520.
- Bloembergen, N. Spin relaxation processes in a 2-proton system. *Phys. Rev.* **1956**, *104* (6), 1542–1547.
- Bloembergen, N.; Morgan, L. O. Proton relaxation times in paramagnetic solutions effects of electron spin relaxation. *J. Chem. Phys.* **1961**, *34* (3), 842–850.
- Solomon, I. Relaxation processes in a system of 2 spins. *Phys. Rev.* **1955**, *99* (2), 559–565.
- Solomon, I.; Bloembergen, N. Nuclear magnetic interactions in the HF molecule. *J. Chem. Phys.* **1956**, *25* (2), 261–266.
- Aime, S.; Crich, S. G.; Gianolio, E.; Giovenzana, G. B.; Tei, L.; Terreno, E. High sensitivity lanthanide(III) based probes for MR-medical imaging. *Coord. Chem. Rev.* **2006**, *250* (11–12), 1562–1579.
- Chan, K. W. Y.; Wong, W. T. Small molecular gadolinium(III) complexes as MRI contrast agents for diagnostic imaging. *Coord. Chem. Rev.* **2007**, *251*, 2428–2451.
- Frullano, L.; Meade, T. J. Multimodal MRI contrast agents. *J. Biol. Inorg. Chem.* **2007**, *12* (7), 939–949.
- Hermann, P.; Kotek, J.; Kubicek, V.; Lukes, I. Gadolinium(III) complexes as MRI contrast agents: Ligand design and properties of the complexes. *Dalton Trans.* **2008**, (23), 3027–3047.
- Major, J. L.; Parigi, G.; Luchinat, C.; Meade, T. J. The synthesis and in vitro testing of a zinc-activated MRI contrast agent. *Proc. Natl. Acad. Sci. U.S.A.* **2007**, *104* (35), 13881–13886.
- Moats, R. A.; Fraser, S. E.; Meade, T. J. A “smart” magnetic resonance imaging agent that reports on specific enzymatic activity. *Angew. Chem., Int. Ed.* **1997**, *36* (7), 726–728.
- Que, E. L.; Chang, C. J. A smart magnetic resonance contrast agent for selective copper sensing. *J. Am. Chem. Soc.* **2006**, *128*, 15942–15943.
- Sherry, A. D.; Woods, M. Chemical exchange saturation transfer contrast agents for magnetic resonance imaging. *Annu. Rev. Biomed. Eng.* **2008**, *10*, 391–411.
- Zhang, X. A.; Lovejoy, K. S.; Jasanoff, A.; Lippard, S. J. Water-soluble porphyrins imaging platform for MM zinc sensing. *Proc. Natl. Acad. Sci. U.S.A.* **2007**, *104* (26), 10780–10785.
- Helm, L.; Merbach, A. E. Water exchange on metal ions: Experiments and simulations. *Coord. Chem. Rev.* **1999**, *187*, 151–181.
- Pidcock, E.; Moore, G. R. Structural characteristics of protein binding sites for calcium and lanthanide ions. *J. Biol. Inorg. Chem.* **2001**, *6* (5–6), 479–489.
- Yang, Z. R.; Batra, R.; Floyd, D. L.; Hung, H. C.; Chang, G. G.; Tong, L. Potent and competitive inhibition of malic enzymes by lanthanide ions. *Biochem. Biophys. Res. Commun.* **2000**, *274* (2), 440–444.
- Burling, F. T.; Weis, W. I.; Flaherty, K. M.; Brunger, A. T. Direct observation of protein solvation and discrete disorder with experimental crystallographic phases. *Science* **1996**, *271* (5245), 72–77.
- Ng, K. K. S.; Kolatkar, A. R.; Park-Snyder, S.; Feinberg, H.; Clark, D. A.; Drickamer, K.; Weis, W. I. Orientation of bound ligands in mannose-binding proteins—Implications for multivalent ligand recognition. *J. Biol. Chem.* **2002**, *277* (18), 16088–16095.
- Allen, M.; Bulte, J. W. M.; Liepold, L.; Basu, G.; Zywicke, H. A.; Frank, J. A.; Young, M.; Douglas, T. Paramagnetic viral nanoparticles as potential high-relaxivity magnetic resonance contrast agents. *Magn. Reson. Med.* **2005**, *54* (4), 807–812.
- Aime, S.; Botta, M.; Terreno, E. *Gd(III)-Based Contrast Agents for MRI*; Elsevier: Amsterdam, The Netherlands, 2005; Vol. 57, pp 173–237.
- Xu, J.; Franklin, S. J.; Whisenhunt, D. W.; Raymond, K. N. Gadolinium complex of tris(3-hydroxy-1-methyl-2-oxo-1,2-didehydropyridine-4-carboxamido)ethylamine—A new class of gadolinium magnetic-resonance relaxation agents. *J. Am. Chem. Soc.* **1995**, *117* (27), 7245–7246.
- $pGd = -\log[Gd]_{free}$ ;  $[Gd]_{total} = 1 \mu M$ ,  $[L]_{total} = 10 \mu M$  (pH 7.4, 25 °C, 0.1 M KCl).
- Werner, E. J.; Datta, A.; Jocher, C. J.; Raymond, K. N. Recent developments in the pursuit of high-relaxivity MRI contrast agents. *Angew. Chem., Int. Ed.* **2008**, *47* (45), 8568–8580.
- Werner, E. J.; Avedano, S.; Botta, M.; Hay, B. P.; Moore, E. G.; Aime, S.; Raymond, K. N. Highly soluble tris-hydroxypyridonate Gd(III) complexes with increased hydration number, fast water exchange, slow electronic relaxation, and high relaxivity. *J. Am. Chem. Soc.* **2007**, *129* (7), 1870–1871.
- Powell, D. H.; Ni Dhubhghail, O. M.; Pubanz, D.; Helm, L.; Lebedev, Y. S.; Schlaepfer, W.; Merbach, A. E. Structural and dynamic parameters obtained from  $^{17}O$  NMR, EPR, and NMRD studies of monomeric and dimeric  $Gd^{3+}$  complexes of interest in magnetic resonance imaging: An integrated and theoretically self-consistent approach. *J. Am. Chem. Soc.* **1996**, *118* (39), 9333–9346.
- Xu, J. D.; Radkov, E.; Ziegler, M.; Raymond, K. N. Plutonium(IV) sequestration: Structural and thermodynamic evaluation of the extraordinarily stable cerium(IV) hydroxypyridonate complexes. *Inorg. Chem.* **2000**, *39* (18), 4156–4164.
- Xu, J.; Churchill, D. G.; Botta, M.; Raymond, K. N. Gadolinium(III) 1,2-hydroxypyridonate-based complexes: Toward MRI contrast agents of high relaxivity. *Inorg. Chem.* **2004**, *43* (18), 5492–5494.
- Cohen, S. M.; Xu, J. D.; Radkov, E.; Raymond, K. N.; Botta, M.; Barge, A.; Aime, S. Syntheses and relaxation properties of mixed gadolinium hydroxypyridonate MRI contrast agents. *Inorg. Chem.* **2000**, *39* (25), 5747–5756.
- Thompson, M. K.; Botta, M.; Nicolle, G.; Helm, L.; Aime, S.; Merbach, A. E.; Raymond, K. N. A highly stable gadolinium complex with a fast, associative mechanism of water exchange. *J. Am. Chem. Soc.* **2003**, *125* (47), 14274–14275.
- Aime, S.; Botta, M.; Crich, S. G.; Giovenzana, G.; Pagliarini, R.; Sisti, M.; Terreno, E. NMR relaxometric studies of Gd(III) complexes with heptadentate macrocyclic ligands. *Magn. Reson. Chem.* **1998**, *36*, S200–S208.
- Doble, D. M. J.; Botta, M.; Wang, J.; Aime, S.; Barge, A.; Raymond, K. N. Optimization of the relaxivity of MRI contrast agents: Effect of poly(ethylene glycol) chains on the water-exchange rates of  $Gd^{III}$  complexes. *J. Am. Chem. Soc.* **2001**, *123* (43), 10758–10759.
- Pierre, V. C.; Botta, M.; Raymond, K. N. Dendrimeric gadolinium chelate with fast water exchange and high relaxivity at high magnetic field strength. *J. Am. Chem. Soc.* **2005**, *127* (2), 504–505.
- Datta, A.; Hooker, J. M.; Botta, M.; Francis, M. B.; Aime, S.; Raymond, K. N. High relaxivity gadolinium hydroxypyridonate—viral capsid conjugates: Nanosized MRI contrast agents. *J. Am. Chem. Soc.* **2008**, *130* (8), 2546–2552.
- Hajela, S.; Botta, M.; Giraudo, S.; Xu, J. D.; Raymond, K. N.; Aime, S. A tris-hydroxymethyl-substituted derivative of Gd-TREN-Me-3,2-HOPO: An MRI relaxation agent with improved efficiency. *J. Am. Chem. Soc.* **2000**, *122* (45), 11228–11229.
- Hajela, S. P.; Johnson, A. R.; Xu, J. D.; Sunderland, C. J.; Cohen, S. M.; Caulder, D. L.; Raymond, K. N. Synthesis of homochiral tris(2-alkyl-2-aminoethyl)amine

- derivatives from chiral  $\alpha$ -amino aldehydes and their application in the synthesis of water soluble chelators. *Inorg. Chem.* **2001**, *40* (13), 3208–3216.
- 42 Hay, B. P.; Werner, E. J.; Raymond, K. N. Estimating the number of bound waters in Gd(III) complexes revisited. Improved methods for the prediction of  $q$ -values. *Bioconjugate Chem.* **2004**, *15* (6), 1496–1502.
- 43 Barrett, T.; Kobayashi, H.; Brechbiel, M.; Choyke, P. L. Macromolecular MRI contrast agents for imaging tumor angiogenesis. *Eur. J. Radiol.* **2006**, *60* (3), 353–366.
- 44 Toth, E.; Helm, L.; Kellar, K. E.; Merbach, A. E. Gd(DTPA-bisamide)alkyl copolymers: A hint for the formation of MRI contrast agents with very high relaxivity. *Chem.—Eur. J.* **1999**, *5* (4), 1202–1211.
- 45 Thompson, M. K.; Doble, D. M. J.; Tso, L. S.; Barra, S.; Botta, M.; Aime, S.; Raymond, K. N. Hetero-tripodal hydroxypyridonate gadolinium complexes: Syntheses, relaxometric properties, water exchange dynamics, and human serum albumin binding. *Inorg. Chem.* **2004**, *43* (26), 8577–8586.
- 46 Anderson, E. A.; Isaacman, S.; Peabody, D. S.; Wang, E. Y.; Canary, J. W.; Kirshenbaum, K. Viral nanoparticles donning a paramagnetic coat: Conjugation of MRI contrast agents to the MS2 capsid. *Nano Lett.* **2006**, *6* (6), 1160–1164.
- 47 Prasuhn, D. E.; Yeh, R. M.; Obenaus, A.; Manchester, M.; Finn, M. G. Viral MRI contrast agents: Coordination of Gd by native virions and attachment of Gd complexes by azide–alkyne cycloaddition. *Chem. Commun.* **2007**, (12), 1269–1271.
- 48 Hooker, J. M.; Datta, A.; Botta, M.; Raymond, K. N.; Francis, M. B. Magnetic resonance contrast agents from viral capsid shells: A comparison of exterior and interior cargo strategies. *Nano Lett.* **2007**, *7*, 2207–2210.
- 49 Valegard, K.; Liljas, L.; Fridborg, K.; Unge, T. The 3-dimensional structure of the bacterial-virus MS2. *Nature* **1990**, *345* (6270), 36–41.
- 50 Aime, S.; Botta, M.; Crich, S. G.; Giovenzana, G.; Pagliarin, R.; Sisti, M.; Terreno, E. NMR relaxometric studies of Gd(III) complexes with heptadentate macrocyclic ligands. *Magn. Reson. Chem.* **1998**, *36*, S200–S208.